

10. Photoprotective devices in PSII

When the Mn-cluster is functionally impaired, positive charge (electron hole) at P680 may accumulate as a result of charge separation due to the absence of ET from the Mn-cluster (See Figure 1-2, right). As a consequence, a triplet state may form at Chl_a in the D1/D2 protein, which finally leads to singlet oxygen that can damage the PSII complex. To avoid this damage, PSII possesses several photoprotective mechanisms.

10.1. Photoprotection by high-potential Q_A form

10.1.1. Photoprotection by shifting E_m(Q_A)

The Mn-cluster is inactive in cells grown in the dark. In this case, it has been suggested that a high-potential Q_A form dominates (Krieger and Weis, 1992; Krieger et al., 1995). Upon illumination, the inactive Mn-cluster is photo-activated and PSII is transformed into a low-potential Q_A form (Johnson et al., 1995). The high-potential Q_A form can also be generated by Ca²⁺ depletion, resulting in removal of the Mn-cluster (Krieger and Weis, 1992; Krieger et al., 1995). The high-potential Q_A form is energetically unfavorable for ET from Q_A to Q_B as compared to the low-potential Q_A form due to a smaller driving force (Figure 10-1-1).

On the other hand, in the high-potential Q_A form the E_m difference between Q_A and Pheo_{D1} increases by 145 mV relative to the low-potential Q_A form (Krieger and Weis, 1992; Krieger et al., 1995). As discussed in ref. (Johnson et al., 1995), in O₂-evolving active PSII (i.e. the low-potential Q_A form) charge recombination of P680⁺Q_A⁻ seems to occur via P680⁺Pheo_{D1}⁻. In the high-potential Q_A form, the corresponding charge recombination process has been suggested to occur directly, not via P680⁺Pheo_{D1}⁻, since the E_m difference between Q_A and Pheo_{D1} is sufficiently large (Johnson et al., 1995) (Figure 10-1-1). This direct charge recombination is physiologically important, especially if PSII is inactive for O₂-evolution. Note that this inactive PSII is still able to accumulate the P680⁺ state.

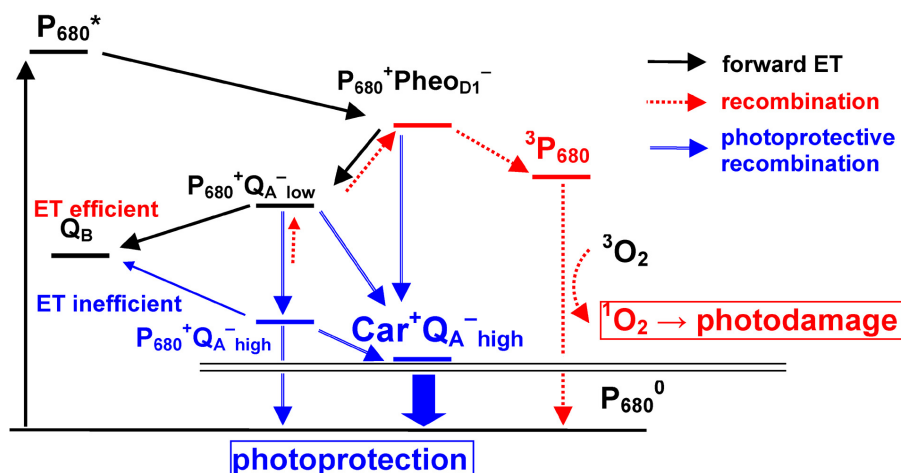


Figure 10-1-1. Energetics of the forward and backward (charge recombination) ET processes in PSII.

The P680⁺Pheo_{D1}⁻ state is known to generate triplet states at P680 with high yield, leading to the harmful singlet oxygen. Thus, the high-potential Q_A form was proposed to play a photo-protective role, since charge recombination of P680⁺Q_A⁻ occurs without involving the triplet generating P680⁺Pheo_{D1}⁻ state (Johnson et al., 1995). The existence of two competing pathways for charge recombination of the P680⁺Q_A⁻ state, originally

proposed for bRC (Gunner et al., 1986; Shopes and Wraight, 1987), is supported by mutational studies varying $E_m(\text{Phe}_{\text{D1}})$ (Rappaport et al., 2002). Indeed, there is a correlation that the lower the $E_m(Q_A)$ leads to photodamage (Krieger-Liszky and Rutherford, 1998).

10.1.2. Varying $E_m(Q_A)$ by flip-flop H bonds

Optimizing hydrogen atom positions for the Q_A^0 state with CHARMM, (Brooks et al., 1983) while fixing all atoms whose coordinates are given by the crystal structure (Ferreira et al., 2004; Loll et al., 2005) (see 2), we confirmed this H-bond pattern (Figure 10-1-2A). We also performed energy optimization of hydrogen atom positions for the Q_A^- state, and found an additional weak H bond from the hydroxyl oxygen of D2-Thr217 to the proximal carbonyl oxygen of Q_A^- (O – O distance 3.7 Å and H – O distance 2.9 Å (Ferreira et al., 2004), Figure 10-1-2B). D2-Thr217 is further H-bonded with the indole nitrogen of D2-Trp253 in both charge states $Q_A^{0/-}$ (Figure 10-1-2).

The calculated $E_m(Q_A)$ was strongly up-shifted from –148 mV in the Q_A^0 state to –52 mV upon the formation of the H bond with D2-Thr217 in the Q_A^- state. Thus, the up-shift in $E_m(Q_A)$ by the H bond with D2-Thr217 amounts to 96 mV, indicating that Q_A^- is significantly stabilized by this newly formed H bond (Ishikita and Knapp, 2005e). All these structural details described above were obtained from the 3.5 Å-structure (Ferreira et al., 2004). Upon the formation of the H bond with D2-Thr217, we observed an up-shift of 107 mV of the computed $E_m(Q_A)$ value in the 3.0 Å-structure (Loll et al., 2005), which is consistent with that calculated in the 3.5 Å-structure. Hereby, the calculated $E_m(Q_A)$ of –10 mV in the 3.0 Å-structure was up-shifted to +97 mV upon H bond formation between Q_A and D2-Thr217 (Ishikita and Knapp, 2005e).

In bRC, the residues corresponding to D2-Thr217 and D2-Trp253 in PSII are fully conserved among *Rb. sphaeroides*, *Rb. capsulatus* and *Blastochloris viridis* (*Bl. viridis*, formerly *Rhodospseudomonas viridis*) (for bRC, see 3.2).

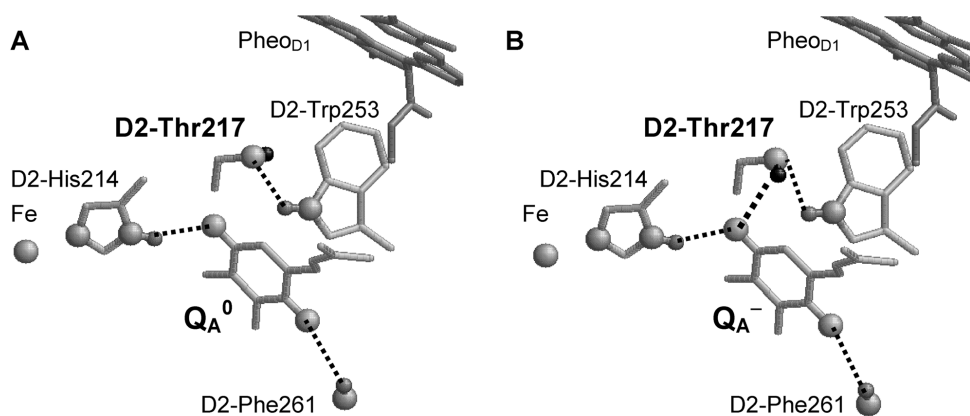


Figure 10-1-2. H-bond pattern of D2-Thr217 at Q_A in PSII. **A)** no H bond in the presence of Q_A^0 ; **B)** H bond (shown as dotted line) stabilized in the Q_A^- state.

10.1.3. Mn-depleted PSII

Krieger *et al.* found that $E_m(Q_A)$ increased by 145 mV upon removal of the Mn-cluster, accomplished by depletion of Ca^{2+} (Krieger and Weis, 1992; Krieger et al., 1995). Interestingly, the measured increase in $E_m(Q_A)$ for a transition from a O_2 -evolving active PSII to an inactive PSII (Krieger and Weis, 1992; Krieger et al., 1995) is similar to our computed $E_m(Q_A)$ up-shift of about 100 mV upon formation of the H bond between Q_A and D2-Thr217 (see 10.1.2). However, it is unclear to what extent the removal of the Mn-cluster may contribute directly to the measured shift of

$E_m(Q_A)$. To clarify this point, we examined the direct influence of the Mn-cluster on $E_m(Q_A)$ computationally. Removing the Mn-cluster by Ca^{2+} depletion eliminates the influence of these positive charges on $E_m(Q_A)$. The computed direct influence from the charges of the Mn-cluster in the S_0 state up-shifts $E_m(Q_A)$ by +36 mV and $E_m(Q_B)$ by +24 mV. Hence, the depletion of the Mn-cluster results in down-shifts of $E_m(Q_A)$ and $E_m(Q_B)$.

If we add the direct influence of 36 mV from the Mn-cluster and of 96 mV from the H bond of D2-Thr217, the resulting total up-shift of $E_m(Q_A)$ is 132 mV. This is consistent with the shift of 145 mV observed by Krieger et al. (Krieger and Weis, 1992; Johnson et al., 1995; Krieger et al., 1995; Rutherford and Krieger-Liszky, 2001). Thus, the additional H bond from D2-Thr217 may play a photo-protective role by providing an alternative charge recombination pathway of the $P680^+Q_A^-$ state that avoids the triplet generating $P680^+Pheo_{D1}^-$ state (Figure 10-1-1).

10.1.4. Dynamics of the H-bond flip of D2-Thr217

The main factor in $E_m(Q_A)$ regulation is a matter of debate. Here, we attribute the H bond with D2-Thr217 to the major factor controlling the low or high-potential Q_A forms (Ishikita and Knapp, 2005e). If this is the case, then both the low and high-potential Q_A forms should exist also in bRC, because D2-Thr217 in PSII is conserved as Thr-M222 in bRC from *Rb. sphaeroides* (Thr-M220 for *Bl. viridis*). Consistently, recent experimental studies revealed the existence of low and high-potential Q_A forms also in bRC from *Bl. viridis* (Fufezan et al., 2005). We note that, not only in bRC from *Rb. sphaeroides* (Stowell et al., 1997) or in PSII (Ferreira et al., 2004), which contain benzoquinones, but also in bRC from *Bl. viridis* where a naphthoquinone is in the Q_A site, the hydroxyl oxygen of Thr-M220 is at a distance of 3.5 Å from the proximal carbonyl oxygen of Q_A (Baxter et al., 2004). This suggests that H bond flip of the Thr is a common mechanism to control $E_m(Q_A)$ in those photosynthetic proteins.

We consider that the actual driving force of the H bond flip of Thr is the negative charge at Q_A in the $P^+Q_A^-$ state^a (Ishikita and Knapp, 2005e). Once bRC or PSII experience $P^+Q_A^-$ accumulation stabilized over a long time range, they become adapted to the high-potential Q_A form. From $E_m(Q_A)$ measurements of herbicide-treated PSII, Fufezan et al. (Fufezan et al., 2002) found that in bromoxynil-treated PSII the $E_m(Q_A)$ is lower by about 100 mV than that in DCMU-treated PSII (for the structure of DCMU, see Figure 7-2-2). They also measured a shorter lifetime for the $P^+Q_A^-$ state in bromoxynil-treated PSII. Thus, they suggested that the change in $E_m(Q_A)$ and $P^+Q_A^-$ lifetime are connected, (Fufezan et al., 2002) which is consistent with our proposal. Notably, the bromoxynil-treated PSII is significantly more photodamaged than the DCMU-treated PSII, (Fufezan et al., 2002) since in this case the charge recombination pathway goes presumably via the triplet generating $P680^+Pheo_{D1}^-$ state (Johnson et al., 1995) due to the lower $E_m(Q_A)$. In the DCMU-treated PSII, presumably direct charge recombination occurs, without involving $P680^+Pheo_{D1}^-$ state. (Johnson et al., 1995)

One might argue that the accumulation of the $P^+Q_A^-$ state can be promoted also by inhibition of the ET from Q_A to Q_B . In bRC, this refers to an inhibition of the conformational gating step (Graige et al., 1998), the rate-limiting step for the first ET to Q_B . Computational studies (Alexov and Gunner, 1999; Ishikita and Knapp, 2004; Zhu and Gunner, 2005) and recent ENDOR studies (Paddock et al., 2005) suggested that the H-bond flip of Ser-L223 to Q_B plays an important role in the conformational gating step (see 3.1).

^a Here the $P^+Q_A^-$ state can also refer to the $P680^+Q_A^-$ state in PSII.

On the other hand, recent kinetic studies for the charge recombination of the $P^+Q_A^-$ state in bRC suggested that the protein-solvent relaxation stabilizing $P^+Q_A^-$ is independent of the conformational gating step (Francia et al., 2003). This is not in conflict with the H-bond flip mechanism of Thr stabilizing the $P^+Q_A^-$ state proposed in our study (Ishikita and Knapp, 2005e).

10.1.5. Are reorientations of residues relevant for the Q_A^- stabilization?

Other possibilities such as drastic reorientations of residue side-chains near Q_A in response to the formation of the $P^+Q_A^-$ state can be excluded, because the recent crystal structures of Katona et al. for the $P^+Q_A^-$ and $P^0Q_A^0$ states of bRC from *Rb. sphaeroides* (PDB: 2BNS and 2BNP, respectively) revealed essentially the same orientation of residues near Q_A (Katona et al., 2005). The predominant differences between the two bRC crystal structures in the $P^+Q_A^-$ and $P^0Q_A^0$ states are small rearrangements of the residues from Pro-H121 to Thr-H226. They suggested that these structural differences create a net electrostatic force to stabilize the Q_A^- state. (Katona et al., 2005) However, in our computation, the calculated $E_m(Q_A)$ based on the two structures differ only by 13 mV. On the other hand, both structures were able to form the additional H bond from Thr-M222 upon Q_A^- formation with an up-shift of $E_m(Q_A)$ by 43-44 mV (Ishikita and Knapp, 2005e). The only way to account for their results is that the H bond between Q_A and Thr-M222 is present in $P^+Q_A^-$ state but absent in $P^0Q_A^0$ state. This interpretation could be hardly obtained solely from the analysis of the crystal structures, in which hydrogen atoms are principally invisible.

Conclusion:

Formation of an H-bond of D2-Thr217 with Q_A stabilizes Q_A^- and up-shifts $E_m(Q_A)$ by ~100 mV, which is consistent with the E_m difference between high-potential and low-potential Q_A forms. This is likely the main mechanism for the formation of a photoprotective, high-potential Q_A form.

10.2. Photoprotection by β -carotene near D2 protein (Car_{D2}), Chl_Z and cytochrome b_{559}

10.2.1. Electron hole transfer from $P680^+$ to $cyt\ b_{559}/Chl_Z$

When water oxidation in PSII is impaired, an alternative ET pathway connecting cytochrome b_{559} ($cyt\ b_{559}$) with $P680^+$ via one of the two Chl_Z (see Figure 1-2), antenna Chl_a and Car is operative. Originally, a simple electron hole transfer pathway according to the scheme 10-1 was assumed (Thompson and Brudvig, 1988; Koulougliotis et al., 1994).

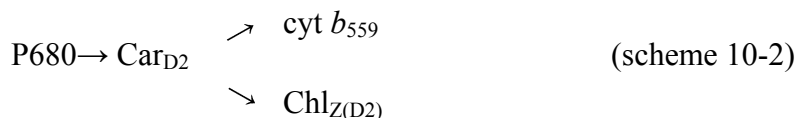


10.2.2. Involvement of Car_{D2} in the pathway

On the other hand, the observation of redox-active β -carotene (Car) in PSII (Hanley et al., 1999; Faller et al., 2001; Tracewell and Brudvig, 2003) leads to another model, involving these Car in the electron hole transfer pathway. The corresponding Car is highly likely the Car near D2 protein (Car_{D2}), or possibly the Car nearby (Car -112 in the recent crystal structure of PSII (Loll et al., 2005)) (see Figure 10-2-1 and 10-3-1). This model places Car at the branch point of two pathways (scheme 10-2), where the electron hole transfer to $cyt\ b_{559}$ is likely to be faster than to Chl_Z (Hanley et al., 1999; Faller et al., 2001) such that the electron hole transfer to Chl_Z is effective only if $cyt\ b_{559}$ is

oxidized.

Indeed, based on the crystal structure at 3.0 Å resolution (Loll et al., 2005) the calculated values are $E_m(\text{Car}_{D2}) = +914$ mV, $E_m(\text{Car-112}) = +955$ mV, $E_m(\text{Chl}_{Z(D1)}) = +1002$ mV and $E_m(\text{Chl}_{Z(D2)}) = +878$ mV (Ishikita and Knapp, 2005a). Remarkably, the calculated $E_m(\text{Car}_{D2})$ and $E_m(\text{Chl}_{Z(D2)})$ are in the same level, indicating that a cationic state can be delocalized between the two cofactors, agreement with scheme 10-2 (see Figure 10-2-1 and 10-3-1).



The E_m of *cyt* b_{559} in PSII is $\sim +400$ mV (Roncel et al., 2003), which is a drastically lower value compared to the E_m for the $\text{Chl}_{Z(D2)}$ and Car_{D2} involved in electron hole transfer. Hence, the formation of Car^+ or Chl_Z^+ can be observed only in the presence of oxidized *cyt* b_{559} . Even under these circumstances, Car^+ is detected only at low temperatures (20 K), while Chl_Z^+ is predominantly observed at elevated temperatures. The latter may be due to the same E_m level of Car_{D2} and $\text{Chl}_{Z(D2)}$ (entropy effect).

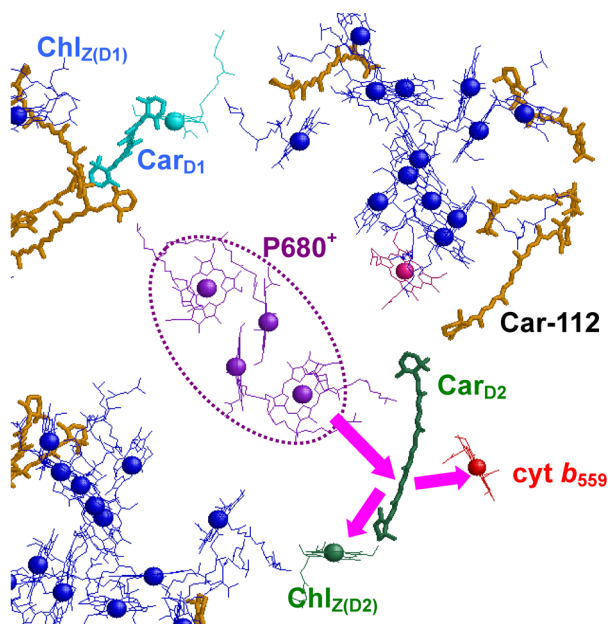


Figure 10-2-1. Electron hole transfer pathway via Car_{D2} .

Scheme 10-2 (Hanley et al., 1999; Faller et al., 2001) suggests that the trapping of Car^+ at low temperature is due to the more rapid electron hole transfer from Car_{D2} to *cyt* b_{559} as compared to the competing transfer to $\text{Chl}_{Z(D2)}$, the latter requiring thermal activation. The electron hole can be shared among these *Car* and *Chl* a , which increases the overall entropy of the electron hole state and explains the temperature dependencies. Thus, an electron hole localized at P680^+ can be quickly transferred to the reduced *cyt* b_{559} via Car_{D2} (or possibly *Car-112*) or trapped by those *Chl* a or *Car*, if *cyt* b_{559} is oxidized (Figure 10-2-1).

These results demonstrate that with a suitable protein environment chemically identical *Chl* a are ready to play very diverse functional roles as there are participation in the ET chain of the RC, in excitation transfer of the light-harvesting antenna system and in P680^+ cation quenching occurring in the antenna subunits. The latter may also serve

as an intermediate storage device of the electron hole in a photo-protection mode of PSII (Ishikita and Knapp, 2005a).

Conclusion:

The calculated E_m for Chl a and Car in the interface between RC and antenna complexes are at the same level but lower than those of $P_{D1/D2}$ and Chl $_{Z(D2)}$, indicating that they form the electron hole transfer pathway from RC to either cyt b_{559} or Chl $_Z$.

10.3. Photoprotection by β -carotene near D1 protein (Car $_{D1}$)

10.3.1. Car $_{D1}$ and Car $_{D2}$

To avoid photodamage, β -carotene (Car) and antenna Chl a play an important role in ET to $P680^+$. In this pathway, a Car $_{D2}$ molecule near Chl $_{Z(D2)}$ is an initial electron donor to $P680^+$, and the donor to Car $_{D2}^+$ is either cytochrome (cyt) b_{559} or Chl $_{Z(D2)}$ when cyt b_{559} is in the reduced (cyt b_{559}^0) or oxidized state (cyt b_{559}^+) (see (10.2.)).

On the other hand, the existence of the corresponding Car in or near the D1 protein (Car $_{D1}$) was proposed mainly from IR spectroscopic studies. There are two Car in PSII that are clearly distinguishable, namely Car $_{489}$ and Car $_{507}$. The former absorbs in the visible at 489, 458 and 429 nm while the latter absorbs at 507, 473 and 443 nm (van Dorssen et al., 1987; Kwa et al., 1992; Tomo et al., 1997; Telfer, 2002; Telfer et al., 2003; Tracewell and Brudvig, 2003). Tomo et al. suggested that Car $_{489}$ and Car $_{507}$ are Car $_{D1}$ and Car $_{D2}$, respectively (Tomo et al., 1997).

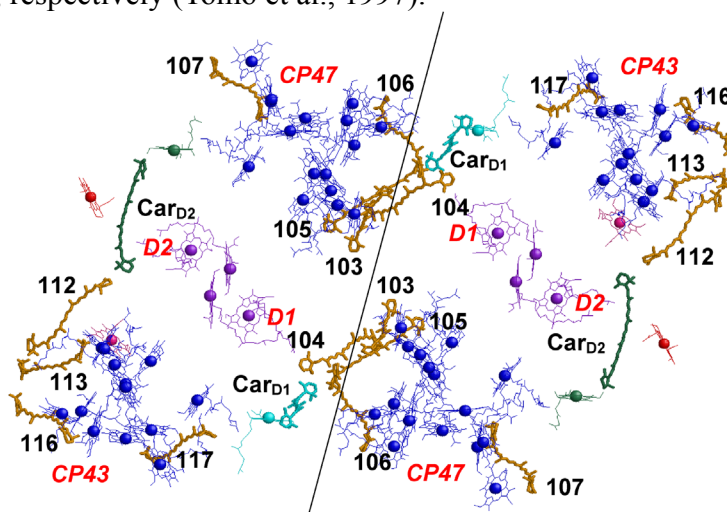


Figure 10-3-1. Location of Car and Chl a in the PSII dimer (Loll et al., 2005). Car $_{D1}$ and Chl $_{Z(D1)}$ are colored in cyan while Car $_{D2}$ and Chl $_{Z(D2)}$ are colored in green. The other Chl a in antenna complex, RC and Car are colored in blue, purple and orange, respectively. The monomer-monomer interface is indicated as solid line.

However, in the former PSII crystal structures at lower resolution Car $_{D1}$ was not observed while one Car (obviously Car $_{D2}$) appears close to cyt b_{559} in all of these crystal structures [two Car per PSII monomer at 3.7 Å resolution (Kamiya and Shen, 2003); seven Car at 3.5 Å resolution (Ferreira et al., 2004); one Car at 3.2 Å resolution (Biesiadka et al., 2004)]. In the crystal structure at 3.0 Å resolution, 11 Car have been revealed per PSII monomer [Loll, 2005 #670] (Figure 10-3-1). This agrees with a recent biochemical evaluation of PSII composition revealing 9 ± 1 Car per PSII monomer (Kern et al., 2005).

10.3.2. Car_{D1} is Car₄₈₉

In the latest crystal structure (Loll et al., 2005), the Car near Chl_{Z(D1)} (Car-101, termed Car_{D1}) is approximately perpendicular to the membrane plane while the Car near Chl_{D2} and Chl_{Z(D2)} (Car-111, termed Car_{D2}) is nearly parallel to the membrane plane (Figure 10-3-2). These orientations of the two Car are identical to those previously proposed for Car₄₈₉ and Car₅₀₇, respectively (van Dorssen et al., 1987; Kwa et al., 1992; Tomo et al., 1997), indicating that these are Car_{D1} and Car_{D2}, respectively. Both Car are at a center-to-center distance of about 36 Å from the non-heme iron in the RC. That distance was estimated to be 38 Å by EPR studies (Lakshmi et al., 2003). In resonance Raman spectra, a difference in two Raman band intensities between Car₄₈₉ and Car₅₀₇ was previously interpreted as the former being in a less stable conformation than the latter (Pascal et al., 1998; Telfer, 2002), which may relate to different Car conformations. However, in the present crystal structure, both Car_{D1} and Car_{D2} are in all-*trans* configuration. Car_{D1} and Chl_{Z(D1)} are both near the PSII monomer-monomer interface. The rather hydrophobic environment of Car_{D1} surrounded by several lipid molecules and another four Car molecules (Car-103, 104, 105 and 106) contrasts with Car_{D2}, whose neighborhood contains only one Car (Car-112) and fewer lipids. This may thus explain the difference in Raman band intensities (Pascal et al., 1998; Telfer, 2002).

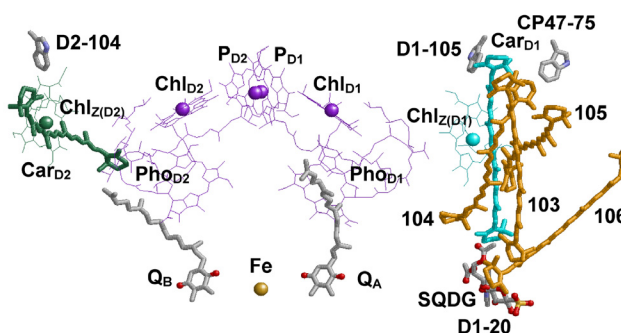


Figure 10-3-2. Location of Car_{D1} (cyan) in the cluster of four Car (orange) with respect to RC (Loll et al., 2005).

In PSII from *Synechocystis* PCC 6803, the redox-active Chl_Z involved in cation quenching was identified as Chl_{Z(D1)} ligated by D1-His118 (Stewart et al., 1998) from EPR and Raman studies. This is in conflict with measurements of fluorescence emission spectra of PSII from *Chlamydomonas reinhardtii*, which pointed to Chl_{Z(D2)} as the ET-active Chl_Z (Wang et al., 2002). In near-IR studies both Chl_{Z(D1)} and Chl_{Z(D2)} can be photooxidized in PSII from spinach (Tracewell et al., 2001), while EPR studies suggested that Chl_{Z(D2)} was the photooxidized one in spinach PSII (Kawamori et al., 2005). The chlorine of Chl_{Z(D1)} being in van der Waals contact with Car_{D1} (edge-to-edge distance 3.7 Å and π - π distance 4.1 Å) also fulfills the requirement for triplet state transfer by spin exchange from ³Chl_{Z(D1)} to Car_{D1}, which in principle could also play a photoprotective role in PSII-RC. But due to the long distances Car_{D1}-Chl_{D1} and Car_{D1}-P_{D1}, Car_{D1} cannot quench the triplet state ³P680 in accordance with spectroscopic results (Takahashi et al., 1987; Durrant et al., 1990; Barber and Archer, 2001).

10.3.3. Involvement of Car_{D1} in photoprotection

The spectroscopically identified Car_{D2} was recently suggested to participate in ET from cyt *b*₅₅₉⁰ to P680⁺ (Faller et al., 2001). This agrees with the PSII crystal structures where cyt *b*₅₅₉ is closer to Car_{D2} than to Car_{D1} (Kamiya and Shen, 2003; Biesiadka et al., 2004; Ferreira et al., 2004). In support, biphasic kinetics of irreversible bleaching was

interpreted as indicating one Car to be more easily oxidized than the other (De Las Rivas et al., 1993), the former presumably being Car_{D2}. As Car⁺ is very unstable in the presence of cyt *b*₅₅₉⁰, Car_{D2}⁺ could not be trapped even at 20 K in PSII-enriched membrane (Hanley et al., 1999). However, in PSII RC samples (consisting of D1, D2 and cyt *b*₅₅₉ proteins, with inactive Y_Z and absent Q_A) oxidation of two Car (presumably Car_{D1} and Car_{D2}) occurs approximately to the same extent (Telfer et al., 2003; Tracewell and Brudvig, 2003). Under more *in vivo* like conditions of PSII-enriched membrane samples (Hanley et al., 1999), oxidation of Car_{D1} seems to be disfavored compared with Car_{D2}. However, it was also suggested that oxidation of Car_{D1} can occur albeit with low quantum yield (Telfer, 2002).

The fact that both Car⁺ can be oxidized in PSII RC samples without Q_A as compared to only one Car⁺ in PSII enriched membranes may be related to the absence of Q_A in the PSII RC samples. In another isolated PSII sub-complex composed of D1, D2, cyt *b*₅₅₉ and CP47 (CP47-RC), Q_A was found only in the CP47-RC dimer, but not in the monomer (Zheleva et al., 1998). Here it was demonstrated that Q_A in CP47-RC dimer helps to reduce the frequency of P680⁺ charge recombination (Bianchetti et al., 1998), lowering the yield of ³P680 formation (Büchel et al., 1999). Since Car cannot quench ³P680 generally (Takahashi et al., 1987; Durrant et al., 1990; Barber and Archer, 2001), elimination of the intermediate charge state prior to ³P680 (i.e. P680⁺Pheo_{D1}⁻ or P680⁺Q_A⁻) is needed to occur in the CP47-RC dimer (Figure 10-1-1). This suggests that the reduced susceptibility to photodamage of the CP47-RC dimer can be attributed to the presence of Q_A (Büchel et al., 1999), which is able to eliminate P680⁺ by charge recombination prior to the formation of ³P680 (then Q_A should be in the high-potential form (Krieger and Weis, 1992; Johnson et al., 1995; Krieger et al., 1995; Ishikita and Knapp, 2005e)).

Even in the more complete PSII complexes that include Q_A e.g. PSII enriched membranes, P680⁺Car_{D1}⁰Q_A⁻ may decay to the ground state via the intermediate P680⁰Car_{D1}⁺Q_A⁻ with low quantum yield. Indeed, a slightly lower quantum yield of 13% cyt *b*₅₅₉⁺/Q_A⁻ with respect to 5% Car⁺/Q_A⁻ in the PSII enriched membranes was interpreted as charge recombination occurring, at least in part, via P680⁰Car⁺Q_A⁻ (Faller et al., 2001). The Car⁺ taking part in the intermediate state is generally considered as Car_{D2}⁺ due to the occurrence of cyt *b*₅₅₉⁺. If we consider that in PSII RC samples Car_{D1}⁺ is highly likely (Telfer et al., 2003; Tracewell and Brudvig, 2003), a transient formation of Car_{D1}⁺ may also be possible in the PSII enriched membranes as previously suggested by Telfer (Telfer, 2002). Placing Car⁺ near cyt *b*₅₅₉⁺ (i.e. D2 side) should be energetically more unstable than to place Car⁺ near Q_A⁻ in the D1 side, although the energy difference may not be so crucial.

In O₂-evolving active PSII with Q_A in the low-potential form, charge recombination of P680⁺Q_A⁻ seems to occur via P680⁺Pheo_{D1}⁻ (Johnson et al., 1995). The P680⁺Pheo_{D1}⁻ state is known to generate triplet states at P680 with high yield. In this sense, the formation of Car_{D1}⁺ is advantageous not only to deprive a positive charge from P680 but also to facilitate the direct charge recombination via P680⁰Car⁺Q_A⁻. If Q_A⁻ of P680⁰Car⁺Q_A⁻ is in the high-potential form (Krieger and Weis, 1992; Johnson et al., 1995; Krieger et al., 1995), the charge recombination via P680⁰Car⁺Q_A⁻ can be more favorable than via P680⁺Pheo_{D1}⁻, since under these circumstances backward ET from Q_A⁻ to Pheo_{D1} becomes inefficient due to the enhancement of the E_m difference between Q_A and Pheo_{D1} by an up-shift of E_m(Q_A).

From the new structure, it became evident that both Car_{D1} and Car_{D2} are surrounded by a number of Trp-residues, namely D1-Trp20, D1-Trp105, CP47-Trp75 with edge-to-edge distances from Car_{D1} of 4.2 Å, 3.5 Å, 4.2 Å, and for Car_{D2} D2-Trp104

with an edge-to-edge distance of 4.0 Å. As both Car show this similar surrounding, a similar photochemical importance for Car_{D1} compared to the one proposed for Car_{D2} (Deligiannakis et al., 2000) can be assumed.

10.3.4. Cluster of Car near Car_{D1}

A cluster of four Car (Car-103, Car-104, Car-105 and Car-106) connects Car_{D1} at the PSII monomer with the antenna Chl_a in CP47 of the adjacent monomer (Figure 10-3-2). Except for Car-105 ($E_m(\text{Car-105}) = +1124$ mV) that is approximately parallel to the membrane plane, the three Car, Car-103, Car-104 and Car-106 have the same calculated level of $E_m(\text{Car})$ (+1043 mV, +1012 mV and +971 mV for PSII monomer-1, respectively, see Table 1) as $E_m(\text{Car}_{D1})$ (Ishikita et al., 2005a). Car-103 and Car-104 are in van der Waals contact, while Car-106 is not. However, Car-106 is in van der Waals contact with Chl_a-29 axially coordinated by CP47-His114 in the adjacent PSII monomer. This Chl_a has been suggested to absorb at significantly longer wavelength of 690 nm as compared to 680 nm for P680 (Shen and Vermaas, 1994).

A direct charge recombination of Car_{D1}⁺Q_A⁻ seems possible (edge-to-edge distance 23 Å and π - π distance 25 Å), but charge recombination of Car-104⁺Q_A⁻ might occur with higher yield due to the proximity of Q_A to Car-104 (edge-to-edge distance 16 Å and π - π distance 17 Å). Unlike Car_{D1}, which is orthogonal to the membrane plane, the axis of Car-104 is oriented more parallel to the membrane plane. Furthermore, in contrast to Car_{D1}, Car-104 has a negatively charged SQDG-13 lipid in its neighborhood and is not surrounded by Trp. Due to the similarity of the calculated E_m of +1002 mV for Car_{D1} and of +1012 mV for Car-104 (Ishikita et al., 2005a), there is no indication of a large energy barrier for ET between the two Car. If we use the E_m difference between Car-104 and Q_A of 1 V and the edge-to-edge distance of 16 Å, the kinetic equation of Page et al. (Page et al., 1999) yields an inverse rate (i.e. lifetime of Q_A⁻) of a few μ s for the ET from Q_A⁻ to Car_{D1}⁺ (4 μ s and 7 μ s based on reorganization energies of 1.2 V and 0.7, respectively (Ishikita et al., 2005a)), which is roughly 20-30 times shorter than the lifetime of ~150 μ s (Boussac et al., 1992) measured for charge recombination of P680⁺Q_A⁻. It should be noted that, except for photodamaged PSII, Car⁺ is unlikely to be accumulated due to efficient ET from the Mn-cluster to P680⁺. Therefore, Car⁺ is essentially absent in functional PSII, and a charge recombination of Car⁺Q_A⁻ does not compete with the forward ET from Q_A⁻ (preferentially, in the low-potential form) to Q_B. In this connection, the presence of a larger number of Car around Car_{D1} than around Car_{D2} may also explain why the localized oxidation state at Car_{D2} is predominantly detected in contrast to a possible oxidation state at Car_{D1} in PSII enriched membranes (summarized in Ref. (Telfer, 2002)).

Conclusion:

The existence of Car_{D1} near Chl_{Z(D1)} is confirmed by the crystal structure at 3.0 Å resolution (Loll et al., 2005). Each Car_{D1} per PSII monomer is surrounded by another four Car and several lipid molecules. The calculated $E_m(\text{Car}_{D1})$ is as high as those of Chl_{Z(D1)} and Car-104. Due to the wire-like shape, Car-104 is close to Q_A, at a edge-to-edge distance of 16 Å from the Q_A head group. This implies that a direct charge recombination of Car-104⁺Q_A⁻ without involving P680⁺Pheo_{D1}⁻ state may be possible. We propose that Car_{D1}, probably with the contribution from Car-104, can play a photoprotective role in PSII.